

2005 中國航太學會/中華民國航學會聯合學術研討會

投稿範圍： **【請務必圈選】**

熱流

- 空氣動力學 實驗與計算流體力學 燃燒與熱質傳
 噴射推進與渦輪引擎 其他_____

結構

- 航太結構 先進材料 固體力學
 其他_____

導航與控制

- 飛行力學 航太電子及通訊 控制與導引
 全球定位系統 天體力學 旋翼機
 其他_____

民航

- 適航認證 民航法規與制度 航太品保
 飛航及安全管理 航空資訊技術 航空經濟與財務
 民航飛行技術 空域規劃與管理 航太醫學
 其他_____

相關航太科技專題

- 微微衛星系統工程 系統與感測科技教育 微系統科技

題目：Studies of Some Detailed Phenomena of a Low Speed Turbulent Wake Flow Field over a Bluff Body

作者（中文）：鄭育能, 陳季聰, 鄭又齊

作者（英文）：Yih-Nen Jeng, Chi-Tsung Chen, You-Chi Cheng

若投稿論文為國科會研究計畫之成果，請註明國科會計畫編號：
NSC-93 -2212-E006-037

欲參加『年青會員論文』獎或『學生論文競賽』獎競賽者請勾選（至多勾選一項，參賽資格請見徵文啟事）：

- 『年青會員論文』獎
 『學生論文競賽』獎

聯絡人：鄭育能
地址：台南市成大航太系
電話：06-2757575-ext.63685
傳真：06-2389940
E-mail：z6208016@email.ncku.edu.tw

流經一個倒梯形柱體之低速紊流的一些細節研究

Studies of Some Detailed Phenomena of a Low Speed Turbulent Flow over a Bluff Body

Yih Nen Jeng 鄭育能教授

Department of Aeronautics and Astronautics, National Cheng Kung University
Tainan, Taiwan 70101, Republic of China, Email: z6208016@email.ncku.edu.tw

Chi-Tsung Chen 陳季聰

Department of Aeronautics and Astronautics, National Cheng Kung University

You-Chi Cheng 鄭又齊

Department of Electrical Engineering, National Taiwan University

ABSTRACT

Time varying data measured at the wake region of a low speed flow over a bluff body is proven to be turbulent via the Hurst analysis. By using an iterative filter, a data string is decomposed into smooth and high frequency part. With the help of a simple Fast Fourier Transform (FFT) algorithm with a small spectrum error, the continuous wavelet transform, also named as Morlet transform, and modified Hilbert transform are employed to study the insights of the data string. The FFT algorithm gives a band-passed data so that these two transforms give several new information about the flow field. Many wave components with variable amplitudes and frequencies are explicitly shown in the two-dimensional wavelet coefficient plot. It is shown that the wavelet coefficient of the Morlet transform involves certain error. That error induced by the finite data domain can not be easily eliminated by inverse transform so that the enhanced Morlet transform give overall qualitative information of the detailed features. The modified Hilbert transform together with the band-passed data string are employed to study the dominate mode of shedding frequency and several sub-harmonics. Although it is not known how to precisely define the frequency bandwidth of a mode, the energy transformed into and out of a mode can be quantitatively extracted. It is interesting to see that, in the wake flow region, the shedding frequency mode does release energy to other modes and the flow field contains low frequency modulation.

Keywords: Low speed turbulent wake flow, two-dimensional wavelet coefficient plot, energy flow into or out of a mode.

1. INTRODUCTION

After the work about low frequency unsteadiness by Bloor's [1] in 1964, many studies on the low-frequency variations embedded in the vortex shedding process have been followed. Miao et al. [2-4] had performed extensive studies upon the detailed structures and mechanism of vortex shedding at low Reynolds number. In Ref.[5-9] Miao et. al. studied the low frequency modulation for flow over different configurations of bluff bodies, in different ranges of Reynolds numbers. In these studies, the Morlet transform [10,11] and empirical mode decomposition method [12-13] were successfully employed.

Because of the flow fluctuation within the wake region is not easy to be studied, Ref.[6,8,9] employed the empirical mode decomposition method and got many valuable insights. Since the method of empirical mode decomposition is principally basing on the average on the upper and lower envelopes of the data string, it can not arbitrary control the desired frequency range of a mode. In this study, the Morlet transform is enhanced by introducing a band-passed data for every scale function

of the transform [14,15] and iterative filter [16]. Consequently, an overall picture of the time-frequency feature can be got. In order to examine the energy flow in and flow out of a mode, the modified Hilbert transform [12,13,17,18] is employed to find the amplitude of the band-passed data string correctly. In early days, people believed that the turbulent flow is related to the random processes [19,20]. One of these studies is the Hurst analysis [21]. In 1962, Lamperti [22] proved the self-similar theorem of random process. Later Mandelbrot [23] pointed that self-similar property can be properly interpreted by the fractal analysis such that the Hurst analysis can be employed to identify a random process. This study will employed the Hurst analysis to make sure that the flow field studied in Ref.[7] is turbulent.

2. ANALYSIS

Hurst Analysis [21]

Assume that a time series data string $\xi_i = \xi(i\Delta t)$, $i = 0, 1, \dots, N$ is known. The average of the rescaled time-span, $\langle \xi \rangle_\tau$, where $\tau \leq N\Delta t$ is defined as

$$\langle \xi \rangle_\tau = \sum_{i=0}^N \xi_i / \tau \quad (1)$$

The accumulated departure of the rescaled time-span $X(t', \tau)$ corresponding to the different rescale time-span was defined for $t' \leq \tau$ is

$$X(t', \tau) = \sum_{u=1}^{\tau} (\xi_u - \langle \xi \rangle_\tau) \quad (2)$$

Next, the departure scope $R(\tau)$ in the range of τ is $R(\tau) = \max[X(t', \tau)] - \min[X(t', \tau)]$ (3)

The standard deviation is defined as

$$S(\tau) = \left[\frac{1}{\tau} \sum_{t'=\Delta t}^{\tau} [\xi(t') - \langle \xi \rangle_\tau]^2 \right]^{1/2} \quad (4)$$

The normalized departure is defined as R/S . Consequently, the consistent departure was gotten by the definition of R/S . Hurst pointed that the exponent H in the following relation is related to the random process.

$$R/S = (k * \tau)^H \quad (5)$$

where k is a constant. There are three different values of Hurst exponent which are corresponding to three kinds of system status in the region of $0 < H < 1$.

1. The case of $H = 0.5$ means that the experimental system appears in random tendency and stays in the state of a classic Brownian motion (white noise).
2. When $H < 0.5$, it indicates that system is fractional Brownian motion or pink noise and appears an anti-persistent status.
3. When $H > 0.5$, it means that the system is high fractional Brownian motion or black noise and appears a persistent status. It also means that the time series system repeats itself rather than in a fully random procedure. When the system continuously goes on, it will decrease in the next period and/or increase in the subsequent periods. This is a persistent time series system with a tendency of following itself previous behavior.

The Iterative Filter Basing on Gaussian Smoothing

Assume that a discrete data string can be approximated by

$$y(t) = \sum_{n=0}^N b_n \cos\left(\frac{2\pi t}{\lambda_n}\right) + c_n \sin\left(\frac{2\pi t}{\lambda_n}\right) \quad (6)$$

In Ref.[20,21], it was proven that after applying the Gaussian smoothing once, the resulting smoothed data becomes

$$\bar{y}_1(t) \approx \sum_{n=0}^N a(\sigma / \lambda_n) \left\{ b_n \cos\left(\frac{2\pi t}{\lambda_n}\right) + c_n \sin\left(\frac{2\pi t}{\lambda_n}\right) \right\} \quad (7)$$

where $a(\sigma / \lambda_n)$ is the attenuation factor introduced by the smoothing and can be proven numerically that

$$0 \leq a(\sigma / \lambda_n) \approx \exp[-2\pi^2 \sigma^2 / \lambda_n^2] \leq 1 \quad (8)$$

If the high frequency part is repeatedly smoothed by the

Gaussian smoothing method, the results are

$$y'_m = \sum_{n=0}^N [1 - a(\sigma / \lambda_n)]^m \left[b_n \cos\left(\frac{2\pi t}{\lambda_n}\right) + c_n \sin\left(\frac{2\pi t}{\lambda_n}\right) \right]$$

$$\bar{y}(m) = \bar{y}_1 + \bar{y}_2 + \dots + \bar{y}_m = y - y'_m$$

$$= \sum_{n=0}^N A_{n,m,\sigma} \left[b_n \cos\left(\frac{2\pi t}{\lambda_n}\right) + c_n \sin\left(\frac{2\pi t}{\lambda_n}\right) \right] \quad (9)$$

where y'_i and \bar{y}_i are the high frequency and smoothed parts at i th smoothing step. Finally, $\bar{y}(m)$ is the smoothed part and y'_m is the high frequency part.

Suppose that all the waveforms within the range of $\lambda_{c1} < \lambda < \lambda_{c2}$ are insignificantly small. The above mentioned iterative smoothing procedure can be an effective filter to give both the low and high frequency parts [20,21]. The desired parameters σ and number of iteration steps m are solved by the following simultaneous equations.

$$1 - [1 - \exp(-2\pi^2 \sigma^2 / \lambda_{c1}^2)]^m = B_1$$

$$1 - [1 - \exp(-2\pi^2 \sigma^2 / \lambda_{c2}^2)]^m = B_2 \quad (10)$$

where $B_1, B_2 = 0.001, 0.999$ are employed in this study.

Enhanced Morlet Transform

For the data string of Eq.(6), the Morlet transform evaluates the wavelet coefficient by the formula.

$$W(a, \tau) = \frac{1}{\sqrt{a}} \int_{-\infty}^{\infty} y(t) e^{-i6(t-\tau)/a} e^{-(t-\tau)^2/(2a^2)} dt \quad (11)$$

where a is called the scale function of the transform.

With the help of the iterative filter, the FFT algorithm of Ref.[17] is employed to give band-passed data via the following steps. At first, the iterative filter is employed to remove the non-sinusoidal and low frequency parts. Then, the FFT algorithm is used to evaluate spectrum with small error. For a given scale function a , the band-passed spectrum is obtained by weighting the spectrum by a Gaussian function. In fact, from the wavelet coefficient, it can be proven that, the maximum response occurs at the mode with $\lambda_n = a\pi/3$. A typical example is shown in Fig.1. After the band-passed spectrum is obtained, the inverse FFT algorithm is employed to give the band-passed data string for a specific scale function a . It can be proven that the resulting wavelet transform convert data string of Eq.(6) to be

$$\bar{W}(a, \tau, y) \approx \sqrt{\frac{\pi a}{2}} \times$$

$$\left\{ \sum_{n=0}^{\infty} b_n \exp\left[-\left[\frac{a^2}{2} + \frac{T^2}{8\pi^2 a^2}\right] \cdot \left[\frac{2\pi}{\lambda_n} - \frac{6}{a}\right]^2\right] \exp\left[\frac{i2\pi\tau}{\lambda_n}\right] + \right. \quad (12)$$

$$\left. \sum_{n=0}^{\infty} c_n \exp\left[-\left[\frac{a^2}{2} + \frac{T^2}{8\pi^2 a^2}\right] \cdot \left[\frac{2\pi}{\lambda_n} - \frac{6}{a}\right]^2\right] \exp\left[-\frac{i2\pi\tau}{\lambda_n}\right] \right\}$$

Here σ is the window size of the Gaussian function on

spectrum domain and is determined by the relation

$$\sigma_n = c \cdot \max[|k_n - k_{n-1}|, |k_{n+1} - k_n|] \quad (13)$$

for the n -th mode, where $k_n = T_{\text{total}}/\lambda_n$ and c is the user defined parameter of window size. The resulting enhanced continuous wavelet transform shown in Eq.(12) introduces a band-passed window on the Fourier spectrum whose center located at a typical frequency $f_c = 1/\lambda_c = 3/(a\pi)$. Without the extra-window term, the remaining $\exp[-a^2/2]$ covers a larger range for a larger value of f_c . This indicates that a large excessive range of spectrum might be employed to calculate the time-frequency coefficient so that the error might be large too. The band-passed factor of $T^2/(8\pi^2\sigma^2)$ has the effect of reducing the resolution error to certain extend. So far it is not known how to relate the window size, σ , to physics and needs further study.

Modified Hilbert Transform

It was proven in Ref.[25] that, for a data string $x(t)$, the modified Hilbert transform

$$J[x(t)] = \int_{t_1}^{t_2} \frac{\exp[-(t-\tau)^2/(2\sigma^2)]x(\tau)}{\pi(t-\tau) \cdot \text{erf}(\sqrt{2}\pi\sigma)} d\tau \quad (11)$$

is approximately equal to the Hilbert transform $\tilde{x}(t)$ of $x(t)$ with an infinitesimal error whenever σ is large enough. In fact, $J[x(t)]$ can be considered as the imaginary part of $x(t)$. The resulting amplitude and frequency have an obviously smaller error than the original Hilbert transform around boundary point and discontinuities.

3. RESULTS AND DISCUSSIONS

Now the experimental data of Ref.[7] is employed to demonstrate the present modified wavelet transform. The u velocity data was taken from $0.5d$ to $10d$ at 7 downstream locations along the centerline of the blunt body's wake region as shown in Fig.2, respectively, where $d = 32\text{mm}$ is the width of the blunt body and $\text{Re}_d = 16500$ is employed. The location of $0.5-1.5d$ is within the near wake region, $2d$ is approximately at the end of near wake region, while that of $3d$ is at the down stream side of the near wake region. The sampling rate is 500 points/second and measuring time interval is 10 seconds. It means that the minimum resolution of frequency was 0.1Hz and the sampling time interval was 0.002sec. Those shown in Table1 are values of Hurst exponent were found in the range from 0.6405 to 0.7229 with a small variances. From the classification of Hurst analysis, the u velocity data is in the range of $0.5 < H < 1$. In other words, the fluctuation in the flow field is a black noise process. It repeats itself after some intermediate procedures which first decays and then increases and/or vice versa. Therefore, the data is a low speed turbulent wake flow field.

The iterative filter is employed to give smooth part of the data and the resulting high frequency part are considered as u' . Figure.3 shows a typical high frequency and smoothed part of data measured at point A. The corresponding Fourier spectrum evaluated by the FFT algorithm of Ref.[14] is shown in Fig.4. Clearly, if

the smooth part is not removed the spectrum will involve certain low frequency error. In order to examine the overall flow properties, the mean u and u' are calculated, respectively, as

$$\bar{u} = \frac{\Delta t}{U_0 T} \left[\sum_{t=0}^{10 \text{ sec}} u \right], \quad \bar{u}' = \frac{\Delta t}{U_0 T} \left[\sum_{t=0}^{10 \text{ sec}} (u - u_{\text{low freq.}})^2 \right]^{1/2} \quad (12)$$

where $T = 10$ second and $U_0 = 7\text{m/s}$ is the inlet velocity. The resulting mean u and \bar{u}' are shown in Fig.5. It seems that the near wake region is approximately ended at $x = 2d$ where the mean velocity is obviously recovered from about zero velocity to a large fraction of inflow mean velocity and the mean velocity fluctuation suddenly drops to the level of down stream wake region.

It seems reasonable to examine the detailed time-frequency data at points A, D, and F which are locations near the base of bluff body, at downstream side of the near wake region, and at far downstream wake region. The resulting two-dimensional wavelet coefficient plot of point A evaluated by the enhanced Morlet transform are shown in Fig.6 with the window parameter $c = 1$. A different c represents a different mode with different band-width which has different physical meaning. Since this is a first study upon this issue, only the case of $c = 1$ is examined to examine the frequency shift among narrow bandwidth modes. A careful inspection upon these figures reveals the followings.

1. At an instant of $t = \text{constant}$, there are many wave components with different wavelengths merged together to form another wave component. There are wave component splits into several wave components. These shows the energy transform between modes. It seems that this is the first time people can look into the details about a turbulent data string.
2. Every wave component can not persist indefinitely. It may terminate itself or may change the frequency so as to convert to be another wave component which is the energy transform between wave components with significant frequency difference.
3. Frequency shift is seen for several modes. That shows the energy changes between adjacent frequency mode.
4. Every wave component shown in the wavelet coefficient plot represents a stream with velocity fluctuation passing through the region around a measured point. A fluctuation of a wave component may be induced by many finite fluid segments involving a series of small eddies (and hence vortices street in irregular shape). Moreover, the starting and termination of a wave component represent the approach and leaving of a series of eddies, vortex filaments, and non-uniform and oscillatory flow pockets with variable degree of vorticity. As a consequence, the time-frequency plot shows that the flow structure around the measured point is very complicated and changes rapidly.

Those shown in Figs.7 and 8 are the real part plots of

cases D and F with $c = 1$, respectively. Many important features are similar to that shown in Fig.6. The main difference is that the mode of shedding frequency becomes a clear band at the immediate downstream point of the near wake region (see Fig.7) and decays at the downstream location (see Fig.8).

From Eq.(12), it is obvious that along a single $a =$ constant line, the wavelet plot accumulates many information in a region on time and frequency domain which deteriorate the temporal resolution. In order to precisely look into the temporal behavior, the modified Hilbert transform is employed to evaluate the band-passed data string. Now the bandwidth of a band-passed data string can be precisely reflected. Those shown in Fig.9 are the 72Hz band-passed data string, amplitude, and frequency of case A, respectively. After carefully checking all the wavelet coefficient plots, the bandwidths of 0.6, 1.2 and 2.0Hz are suitable to grasp consistent data for all cases. For convenience, the data and amplitude plots are shifted by 0.1 and frequency plot shifted by 10Hz for different bandwidths, respectively. Obviously, a wider bandwidth gives a more complicated wave mode as shown. The amplitude follows the envelope of the data string exactly. It is interesting to see that the frequency oscillation runs over a finite bandwidth of 4Hz which can be clearly seen in the detailed plot. This oscillation is introduced by the insufficient sampling rate such that only about 7 points are employed to resolve a wave length. The kink around $t = 3.8$ seconds of $\sigma = 1.5$ Hz is caused by the error induced by the almost vanishing amplitude. Those shown in Fig.10 are result of the band-passed data string of the first sub-harmonic mode (36Hz). It is interesting to see that the amplitude is larger than that of 72Hz. This reflects that, within the near wake region, the first sub-harmonic mode dominates the flow fluctuation because the shed vortex is not directly rolled into the region around the base of the bluff body. This result consists with the extensive studies of Ref.[8] that the low frequency modulation dominates this zone. The frequency oscillation band is now reduced to be 0.5Hz which reflects the error introduced by using 15 points to resolve a wavelength.

In the turbulent flow studies, it is interested to examine quantitatively the energy and energy variation corresponding to the shedding frequency mode and sub-harmonic modes. The latter issue is related to the energy cascade between modes of different frequency. Although we do not the exact mechanism that an energy flow into a mode is fed from which mode and an energy flow out go to which mode, the total amount of flow into and out of a mode can be calculated from the band-passed spectrum together with the modified Hilbert transform. Those shown in Figs.11 are the energy of different modes with different band-widths with respect to the distance measured from the base of the bluff body. The energy of the first sub-harmonic mode is almost the largest one among all modes in the whole wake region as noted in previous paragraph. At the downstream location

within the near wake region, the energy of the shedding frequency mode gradually increases and up to a maximum at $x = 1.5d$. After the near wake region, its energy gradually decay and attains the smallest values among all the modes shown in the figure. The energy of the second and third sub-harmonic modes have the maximum value at $x = 0.d$ and gradually decay in a oscillatory manner. At the far downstream location, where $x \geq 5d$, the energy of all sub-harmonic modes are competitive with the dominate mode. Up to the location of $x = 10d$, because the high frequency mode has a larger dissipation rate, the sub-harmonic modes dominate the flow which also verify the conclusion of Ref.[8].

Figures.12 show the corresponding rate of energy changes with respect to that of Fig.11. The energy changing rate is estimated by the summation of $|r^2(t + \Delta t) - r^2(t)|$ over the time domain. The energy changing rate is a measure of energy pumping in and out of a mode. The figure shows that the main energy recover is provided by the dominate mode of shedding frequency. A careful inspection upon the data string shown in Fig.9a also verifies this fact. At region of $x = 0.5d$ and d , all the sub-harmonic modes have similar energy changing rate which reflect the level low frequency modulation is significant. Near the end of the near wake region, where $x = 1.5d$, the low frequency modes does not have a large energy change rate, while the first sub-harmonic mode receives energy from the dominate mode to make its energy changing rate attaining a maximum value as shown. In down stream location after the near wake region, the high frequency mode gradually pumps energy back into the low frequency modes and eventually causes the mean velocity recovering to the original U_0 as shown in Fig.5.

The discussion of employing the modified Hilbert transform certainly indicates two valuable rewards:

1. The energy and energy exchanging rate of a mode can be precisely extracted.
2. The resulting variation of both data, amplitude, frequency, energy, and energy changing rate can be employed to explain the existing detailed mechanism.

So far it is not known how to employ a suitable bandwidth of the band-passed data string for both wavelet calculation and mode evaluation via the modified Hilbert transform. However, the above discussion shown that, using several bandwidths, the wavelet coefficient plot, energy and energy changing rate of different modes give many detailed information which can clearly explain many known phenomena.

4. CONCLUSION

The enhanced continuous wavelet transform, modified Hilbert transform and an FFT algorithm with small error are successfully employed to examine a low speed flow over a bluff body. The flow field is proven to be turbulent via the Hurst analysis. Many qualitative details are reflected by the resulting wavelet coefficient plots which are not seen before. By using the modified Hilbert

transform, the amplitude and frequency of a mode of a band-passed spectrum can be precisely evaluated. The quantities of energy and the total energy exchanging rate of a mode can be explicitly calculated. The further work should be addressed on how to relate the window size of the band-passed spectrum to physics so that it can be reasonably defined.

ACKNOWLEDGEMENT

This work is supported by the National Science Council of Taiwan under the grant number NSC-93-2212-E006-037. The authors are also grateful to Prof. Miao of Department of aero. and astro., National Cheng-Kung University for his support of given experimental data and many instructive suggestions.

REFERENCES

1. Bloor, M. S., "The Transition to Turbulence in the Wake of a Circular Cylinder," *J. Fluid Mech.*, Vol.19, pp.290-303 (1964).
2. Miao, J. J., Yang, C. C., Chou, J. H., and Lee, K. R., "Suppression of Low-Frequency Variations in Vortex Shedding by a Splitter Plate Behind a Bluff Body," *J. Fluids and Structures*, Vol.7, pp.897-912 (1993).
3. Miao, J. J., Yang, C. C., Chou, J. H., and Lee, K. R., "A T-shaped Vortex Shedder for a Vortex Flowmeter," *Flow Measurement and Instruments* 4, No. 4, pp.259-267(1993).
4. Miao, J. J., Wang, J. T., Chou, J. H., and Wei, C. Y., "Characteristics of Low-Frequency Variations Embedded in Vortex Shedding Process," *J. Fluids and Structures*, Vol.13, pp.339-359 (1999).
5. Miao, J. J., J. T. Wang, J. H. Chou and C. Y. Wei., "Low-Frequency Fluctuations in the Near-Wake Region of a Trapezoidal Cylinder with Low Aspect Ratio," *Journal of Fluids and Structures* Vol.17/5, pp.701-715 (2003)
6. Hu, C. C., Miao, J. J., and Chau, J. H., "Instantaneous Vortex-Shedding Behaviour in Periodically Varying Flow," *Proc. R. Soc. Lond. A*, Vol. 458, pp. 911-932(2002).
7. Wu, S. J., "Instantaneous Properties of Low-Frequency Modulations and Three-Dimensionality Associated with Vortex Shedding," Ph. D. Dissertation, National Cheng Kung University, June 2003.
8. Miao, J. J., S. J. Wu, C. C. Hu, and J. H. Chou, "Low Frequency Modulations Associated with Vortex Shedding form Flow over Bluff Body," *AIAA J.*, vol.42, no.7, pp.1388-1397, 2004.
9. Wu, S. J., J. J. Miao, C. C. Hu, and J. H. Chou, "On Low-Frequency Modulations an Three-Dimensionality in Vortex Shedding behind Flat Plates," *J. Fluid Mechanics*, vol.526, pp.117-146, 2005.
10. Grossman, A. and Morlet, J., "Decomposition of Hardy Functions into Square Integrable Wavelets of Constant Shape," *SIAM J. Math. Anal.*, Vol. 15, No. 4, 1984, pp. 723-736.
11. Farge, M., "Wavelet Transforms and Their Applications to Turbulence," *Annu. Rev. Fluid Mech.*,

- Vol. 24, 1992, pp. 395-457.
12. Huang, N. E., Z. Shen, and S. R. Long, "A New View of Nonlinear Water Waves: the Hilbert Spectrum," *Annual Reviews of Fluid Mechanics*, 1999, vol.51, pp.417-457.
13. Huang, N. E., Shen, Z., Long, S. R., Wu, M. C., Shih, H. H., Zheng, Q., Yen, N. C., Tung, C. C. and Liu, H. H., "The Empirical Mode Decomposition and the Hilbert Spectrum for Nonlinear and Non-stationary Time Series Analysis," *Proc. R. Soc. Lond. A.*, vol. 454, pp.903-995, 1998.
14. Jeng, and Y. C. Cheng, "A Simple Strategy to Evaluate the Frequency Spectrum of a Time Series Data with Non-Uniform Intervals," *Transactions of the Aeronautical and Astronautical Society of the Republic of China*, vol.36, no.3, pp.207-214, 2004 . Bendat, J. S., and Piersol, A. G., "Random Data Analysis and Measurement Procedures," 3rd ed., John Wiley & Sons, New York, 2000, Chapters 10 & 11, pp.349-456.
15. Jeng, Y. N., C.T. Chen, and Y. C. Cheng, "A New and Effective Tool to Look into Details of a Turbulent Data String," *Proceedings of 12th National Computational Fluid Dynamics Conference*, Kaohsiung, paper no. CFD12-2501, Aug. 2005.
16. Jeng, Y. N., P. G. Huang, and H. Chen, "Filtering and Decomposition of Waveform in Physical Space Using Iterative Moving Least Squares Methods," *AIAA paper no.2005-1303*, Reno Jan. 2005.
17. Bendat, J. S., and Piersol, A. G., *Random Data Analysis and Measurement Procedures*, 2nd ed., John Wiley & Sons, New York, 1986, Chapter 13, pp.484-510.
18. Jeng, Y. N., "Modified Hilbert Transform for Non-stationary Data of Finite Range," 7th National CFD Conference, pp.15-22, Aug. 2000, Taiwan.
19. Richardson, L.F., "Weather prediction by numerical process", (Cambridge Univ. Press, 1922).
20. Kolmogorov, A. N., "The local structure of turbulence in incompressible viscous fluid for very large Reynolds number", *Dokl. Akad. Nauk SSSR* 30, 9 (1941) (Reprinted in *Proc. Royal Soc. London A* 434, 913; 1991).
21. Hurst, H.E., "Long-Term storage in reservoirs", *Trans. Am. Soc. Civ. Eng.* 116, 770 (1965).
22. Lamperti, J.W., "Semi-Stable Processes", *Trans. Am. Math. Soc.* **104**, 62(1962).
23. Mandelbrot, B. B., *Gaussian Self-Affinity and Fractals*, Springer; New York, 2002.

Table 5.1

Average Hurst exponent H and Variance σ of H

	P_h	A	B	C	D	E	F	G
H	0.6882	0.6908	0.708	0.7229	0.7017	0.6405	0.6829	0.6978
σ	0.0233	0.0415	0.0801	0.0121	0.0335	0.0199	0.0188	0.0201

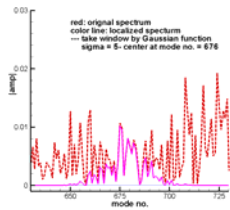


Fig.1 Original and band-passed spectrums: dashed line is the original spectrum and solid line is a band-passed spectrum.

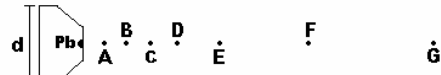


Fig.2 A schematic drawing of wake flow and setup of measuring position, $d = 32$ mm. The locations are: $0.5d$ for A, $1d$ for B, $1.5d$ for C, $2d$ for D, $3d$ for E, $5d$ for F, and $10d$ for G.

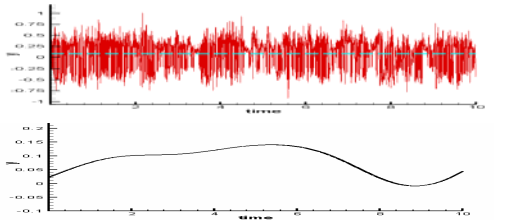


Fig.3 One of the high frequency and smooth parts measured at point A.

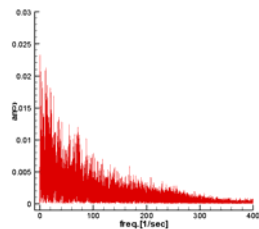


Fig.4 The spectrum of the high frequency part of Fig.2.

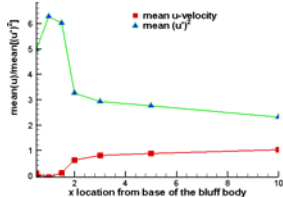


Fig.5 The mean u/U_0 and u'/U_0 velocity measured at different locations.

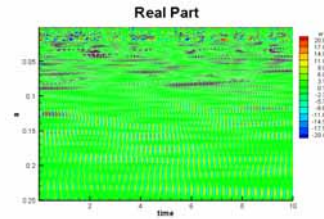
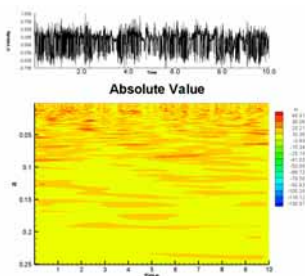


Fig.6 The amplitude and real part of the wavelet coefficient plot of case A, generated by the proposed modified Morlet transform, scale factor of spectrum windowing is $c = 1$.

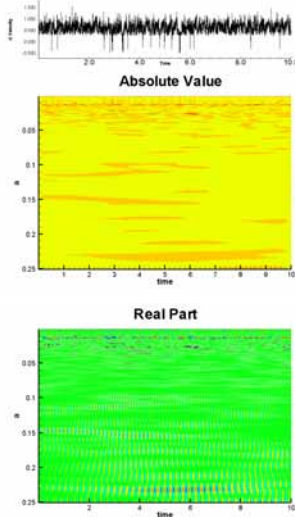


Fig.7 The amplitude and real part of the wavelet coefficient plot of case D, generated by the proposed modified Morlet transform, scale factor of spectrum windowing is $c = 1$.

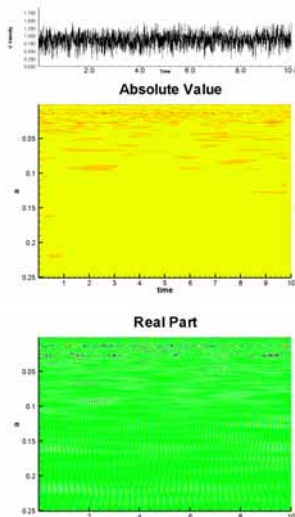


Fig.8 The amplitude and real part of the wavelet coefficient plot of case F, generated by the proposed modified Morlet transform, scale factor of spectrum windowing is $c = 1$.

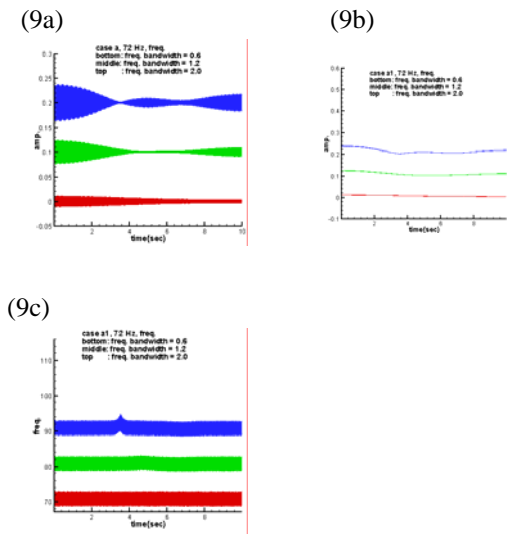


Fig.9 The 72Hz mode of the Case A with different bandwidth: (a) is data; (b) is amplitude; and (c) is frequency. Three bandwidths are employed: 0.3, 1.2 and 1.5 Hz.

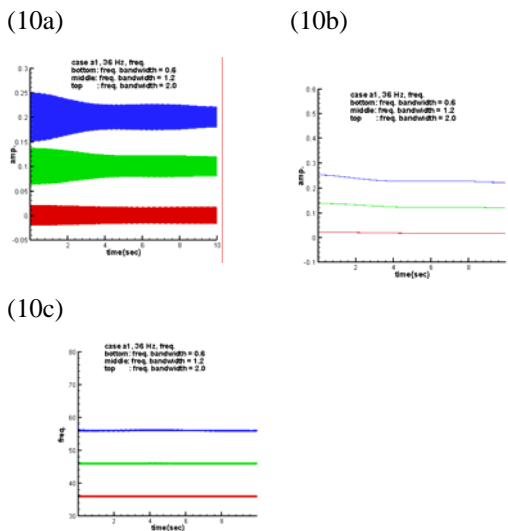


Fig.10 The 36Hz mode of the Case A with different bandwidth: (a) is data; (b) is amplitude; and (c) is frequency. Three bandwidths are employed: 0.3, 1.2 and 1.5 Hz.

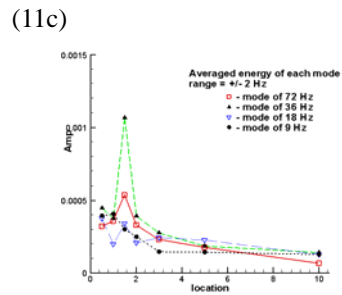
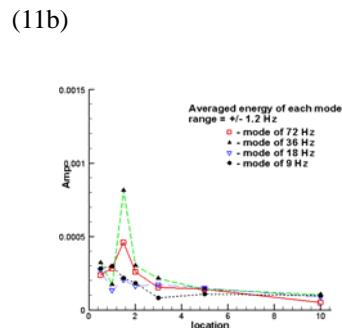
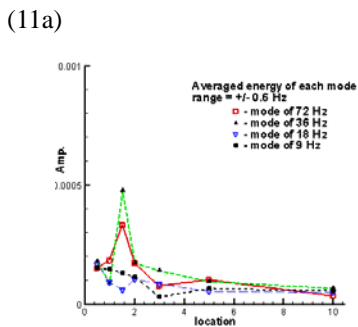


Fig.11 The mean energy of different modes at different measured location: (a) uses a bandwidth of 0.6Hz; (b) uses 1.2Hz; and (c) uses 2Hz.

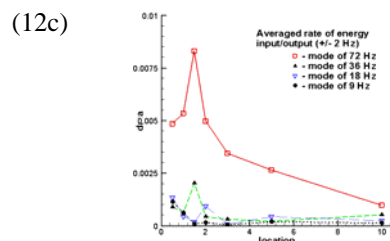
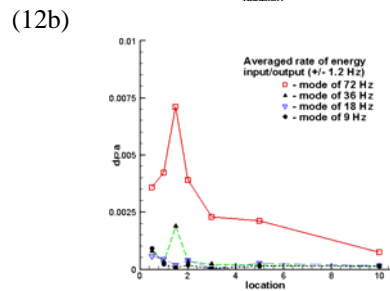
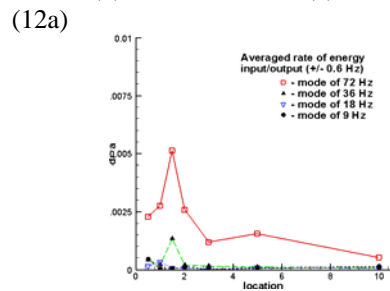


Fig.12 The mean energy variation of different modes at different measured location: (a) uses a bandwidth of 0.6Hz; (b) uses 1.2Hz; and (c) uses 2Hz.

流經一個倒梯形柱體之低速紊流的 一些細節研究

鄭育能教授
國立成功大學航太系
陳季聰
國立成功大學航太系博士生
鄭又齊
台大電機系畢業生

摘要

本文使用低誤差的簡易快速傅立葉轉換式產生正確的頻譜和帶狀濾波數據，配合強化的 Morlet 小波轉換公式及修正型 Hilbert 轉換，探討流經一倒梯形鈍頭體的低速尾流。該流場使用 Hurst 分析法證明為紊流。強化的 Morlet 小波轉換產生小波係數圖能夠顯示清晰的二維時頻關係。使用修正型 Hilbert 轉換則可將數個流場主頻和諧頻波的振幅和頻率正確的解析，並因而正確的算出每一主、諧頻的能量和能量交換量，用以解釋已知的低頻之調頻行為模式。

關鍵詞：強化的 Morlet 小波轉換公式，修正型 Hilbert 轉換，時頻分析，低速紊流，低頻調頻